

Simulation of Optical Resonance Filters Using Wavelet Homogenization

Per-Olof Persson (pop@nada.kth.se), NADA, KTH
Thesis advisor: Professor Björn Engquist

May 12, 1997

Abstract

The simulation of optical resonance filters based on quarter-wave shifted waveguide gratings is described. Wavelet-based numerical homogenization is applied to the filters, and the properties of the homogenized operators and their solutions are investigated. A method is proposed for replicating periodical sub-structures in the homogenized operators, making it possible to model very large structures with moderate computational effort.

Contents

| | | |
|----------|---|-----------|
| 1 | Introduction | 1 |
| 2 | Time-harmonic solutions to the wave equation | 2 |
| 2.1 | The Helmholtz equation | 2 |
| 2.2 | Discretization of the Helmholtz equation | 3 |
| 2.3 | Boundary conditions | 4 |
| 3 | Simulation of optical filter | 5 |
| 3.1 | The grating resonance filter | 5 |
| 3.2 | Approximation in one dimension | 6 |
| 3.3 | Two-dimensional calculations | 8 |
| 4 | Wavelet homogenization | 9 |
| 4.1 | Theory | 9 |
| 4.2 | Homogenization of optical filter | 12 |
| 4.3 | Extending periodical structures | 14 |
| 4.4 | Homogenization in two dimensions | 16 |
| 5 | Conclusions | 17 |
| 6 | Acknowledgements | 18 |
| | References | 19 |

1 Introduction

In this report, I present the numerical simulation of an optical filter. The filter consists of a waveguide with two gratings separated by a small displacement. A wave with the specific resonant frequency will be transmitted when sent through the filter, while waves with the adjacent frequencies will be reflected.

The design of the filter determines many of its interesting properties, for instance the value of the resonant frequency and the sharpness of the resonance peak. Design parameters of interest are, for example, the geometry of the gratings, the number of etches, the materials used and the width of the waveguide. It is of great interest to simulate the filter numerically in order to anticipate the influence of these parameters.

The calculations of a wave interacting with the waveguide gratings in the filter can be very complicated. The geometry needs to be described in at least two dimensions, and the number of etches in the gratings is very large. Furthermore, in order to accurately model the interference between the reflected waves, a high resolution is needed.

In order to make the computations more efficient, I have studied the advantages of using wavelet homogenization. This technique makes it possible to compute the solution on a coarse grid without losing the influence of the fine-scale details. For the optical filter, the individual etches can be very accurately represented without making the final solution process more difficult.

As we will see, it is not necessary to homogenize the complete filter. Since the gratings are periodical repetitions of etches with identical geometry, the homogenized operator will be periodical as well. Thus it is sufficient to homogenize a few etches, and by replicating them it is easy to construct the operator representing the whole filter. Using this technique, I have been able to simulate filters with a very large number of high-detail etches on an ordinary workstation. The high resolution facilitates, for example, the analysis and the optimizations of complex grating-geometries¹.

Wavelet homogenization can be used in the same way in other applications to make computations more efficient. Examples are the studies of antenna-arrays and anti-reflection coatings, both having periodical substructures that need to be resolved in detail.

Most of the calculations in this work have been made in MATLAB 5.0 on a Sun Ultra 1 workstation. However, to be able to perform the computations on the large two-dimensional filters in Section 3.3 (without homogenization), the code was rewritten in C++. This made it possible to use "Strindberg", the IBM SP2 parallel computer at PDC, to obtain very high calculation

¹Today, the grating fabrication process is limited to produce rectangularly shaped gratings [11], but an optimization would be of theoretical interest.

speeds.

I have exclusively used *gaussian elimination* to solve the banded linear systems that arise from the discretizations. To reduce the memory requirements, I made an implementation of the *biconjugate gradients* method as well. In practice, I never used this iterative solver because of its longer execution time.

This report consists of three parts. The mathematics needed for the simulations is given in Section 2. The actual calculations on the optical filters and the properties of the solutions are presented in Section 3, and finally in Section 4 the theory of the wavelet homogenization and its application on the filters are shown. The report ends with a short concluding section.

2 Time-harmonic solutions to the wave equation

The governing equation in the simulation of wave propagation is the *wave equation*, which can be written

$$\psi_{tt} = c^2 \nabla \cdot (a \nabla \psi), \quad a = \left(\frac{v}{c}\right)^2 \quad (1)$$

where the *propagation velocity* v is permitted to vary in space and c is a reference velocity. The dimensionless quantity a is introduced in order to simplify the equations later on.

2.1 The Helmholtz equation

In the modeling of wave propagation, scattering and interference phenomena, the detailed time-dependence in the solutions of (1) is often of less interest, and the calculations can be simplified by seeking time-harmonic solutions. Assume the solution $\psi(\mathbf{x}, t)$ oscillates with the same fixed angular frequency ω at all points in space,

$$\psi(\mathbf{x}, t) = u(\mathbf{x}) \cdot e^{i\omega t}. \quad (2)$$

Substitution into the wave equation (1) gives

$$-\omega^2 u(\mathbf{x}) \cdot e^{i\omega t} = c^2 \nabla \cdot (a(\mathbf{x}) \nabla u(\mathbf{x})) \cdot e^{i\omega t} \quad (3)$$

and finally, with the *wave number* $k = \omega/c$,

$$\nabla \cdot (a \nabla u) + k^2 u = 0. \quad (4)$$

This time independent partial differential equation is known as the *Helmholtz equation*.

2.2 Discretization of the Helmholtz equation

To solve the Helmholtz equation numerically, it must first be discretized. In one dimension, (4) becomes

$$\frac{d}{dx} \left(a(x) \frac{d}{dx} u(x) \right) + k^2 u(x) = 0. \quad (5)$$

Introduce a grid of $N + 2$ equally spaced points $\{x_i\}$ such that

$$x_i = x_{\text{in}} + (i - 1/2)h, \quad \begin{cases} i = 0, \dots, N + 1, \\ h = (x_{\text{out}} - x_{\text{in}})/N. \end{cases} \quad (6)$$

The gridfunctions corresponding to $u(x)$ and $a(x)$ can then be defined as

$$\begin{aligned} u_i &\approx u(x_i), & i &= 0, \dots, N + 1, \\ a_{i+1/2} &= a(x_i + h/2), & i &= 0, \dots, N. \end{aligned} \quad (7)$$

When discretizing the derivatives, they are replaced by central difference approximations according to

$$\frac{d}{dx} f(x) \approx \frac{f(x + \frac{h}{2}) - f(x - \frac{h}{2})}{h}. \quad (8)$$

Now, the discretization of (5) becomes

$$\frac{1}{h} \left(a_{i+1/2} \frac{u_{i+1} - u_i}{h} - a_{i-1/2} \frac{u_i - u_{i-1}}{h} \right) + k^2 u_i = 0, \quad i = 1, \dots, N \quad (9)$$

or, equivalently,

$$a_{i+1/2} u_{i+1} - (a_{i+1/2} + a_{i-1/2}) u_i + a_{i-1/2} u_{i-1} + h^2 k^2 u_i = 0, \quad i = 1, \dots, N. \quad (10)$$

This can be written as a tridiagonal linear system of equations,

$$Lu = f, \quad (11)$$

where $u = (u_1, \dots, u_N)^T$ and f is a vector determined by the boundary conditions (see Section 2.3).

Extending the discretization to higher order space dimensions is straightforward. In two dimensions, the y -axis is discretized with $M + 2$ points in the same manner as in (6). Define the gridfunction corresponding to $u(x, y)$ as

$$u_{i,j} \approx u(x_i, y_j), \quad \begin{cases} i = 0, \dots, N + 1, \\ j = 0, \dots, M + 1, \end{cases} \quad (12)$$

and similarly for $a(x, y)$. Assuming the same grid-spacing h in both dimensions, the discretization of the Helmholtz equation becomes

$$\begin{aligned} &a_{i+1/2,j} u_{i+1,j} - (a_{i+1/2,j} + a_{i-1/2,j}) u_{i,j} + a_{i-1/2,j} u_{i-1,j} \\ &+ a_{i,j+1/2} u_{i,j+1} - (a_{i,j+1/2} + a_{i,j-1/2}) u_{i,j} + a_{i,j-1/2} u_{i,j-1} + h^2 k^2 u_{i,j} = 0. \end{aligned} \quad (13)$$

Also in two dimensions this corresponds to a sparse linear system of equations, similar to (11).

2.3 Boundary conditions

In the simulation of a wave propagating through a fiber, it is important that no reflections arise at the boundaries of the computational region. To achieve this, *non-reflecting boundary conditions* must be used.

Assume the one-dimensional solution $u(x)$ to be composed of two waves, $u_{\rightarrow}(x) = e^{-ikx}$ and $u_{\leftarrow}(x) = e^{ikx}$, propagating in the positive and the negative x -direction respectively. The condition that there should be no reflection at the boundary where the wave leaves the domain can be expressed as

$$u(x) = Tu_{\rightarrow}(x), \quad x \approx x_{\text{out}}, \quad (14)$$

where T is the transmitted amplitude. Differentiation of (14) gives the first boundary condition,

$$\frac{d}{dx}u(x) + iku(x) = 0, \quad x = x_{\text{out}}. \quad (15)$$

At the boundary where the wave enters the domain, the solution consists of the incoming wave with the amplitude 1 and a reflected wave with the (unknown) amplitude R ,

$$u(x) = 1 \cdot u_{\rightarrow}(x) + R \cdot u_{\leftarrow}(x), \quad x \approx x_{\text{in}}. \quad (16)$$

Differentiation of (16) and elimination of R gives,

$$\begin{aligned} \frac{d}{dx}u(x) &= -1 \cdot iku_{\rightarrow}(x) + R \cdot iku_{\leftarrow}(x) \\ &= -1 \cdot iku_{\rightarrow}(x) + ik \cdot (u(x) - 1 \cdot u_{\rightarrow}(x)) \\ &= -2 \cdot iku_{\rightarrow}(x) + iku(x) \end{aligned} \quad (17)$$

and the second boundary condition becomes

$$\frac{d}{dx}u(x) - iku(x) = -2ike^{-ikx}, \quad x = x_{\text{in}}. \quad (18)$$

The relations (18) and (15) are discretized as

$$\begin{aligned} \frac{u_1 - u_0}{h} - ik \frac{u_1 + u_0}{2} &= 2ike^{-ikx_{\text{in}}}, \\ \frac{u_{N+1} - u_N}{h} + ik \frac{u_{N+1} + u_N}{2} &= 0, \end{aligned} \quad (19)$$

which after simplification becomes

$$\begin{aligned} (2 + ihk)u_0 - (2 - ihk)u_1 &= 4ihke^{-ikx_{\text{in}}}, \\ (2 + ihk)u_{N+1} - (2 - ihk)u_N &= 0. \end{aligned} \quad (20)$$

The intensity I_{tr} of the transmitted wave is given by

$$I_{\text{tr}} = |u(x_{\text{out}})|^2 \approx |u_N|^2. \quad (21)$$

In two dimensions, the same non-reflecting boundary conditions are used at the left and right boundary of the domain. There must also be boundary conditions for the top and bottom of the waveguide. In this case I will use a *Neumann condition*, $du/dn = 0$, which is discretized as

$$\begin{cases} u_{i,0} = u_{i,1}, \\ u_{i,M+1} = u_{i,M}, \end{cases} \quad i = 1, \dots, N. \quad (22)$$

For the boundary conditions (15) and (18) to be accurate in higher space dimensions, it is important that the wavefront is planar at the input and output boundaries, and that the incidence is normal. As we will see later, this is almost true in my simulations of optical fibers. The transmitted intensity I_{tr} is then calculated as an integral over the cross-section at the output boundary Γ_{out} ,

$$I_{\text{tr}} = \int_{\Gamma_{\text{out}}} |u|^2 dS \approx h \sum_{j=1}^M |u_{N,j}|^2. \quad (23)$$

3 Simulation of optical filter

An optical filter is a device that distinguishes a specific frequency of light from the adjacent frequencies. It can be used in optical fiber communication, where information is sent at multiple frequencies through the same waveguide in order to get a larger bandwidth. At the end of the communication line, filters are used to separate the information.

3.1 The grating resonance filter

In the *grating resonance filter*, the wave to be filtered is sent through a waveguide with grating etches. The etches are equally spaced, except for a quarter-wave step somewhere in between, see Figure 1 (left). This causes the resonant wavelength $\lambda_{\text{res}} = 2\Lambda n_{\text{eff}}$ to pass through while the adjacent wavelengths are filtered out. Here Λ is the grating spacing and n_{eff} is the effective index of refraction.

Actually, the etches can be replaced by anything that reflects a small portion of the wave, for example as in the *Fabry-Perot interference filter* [8] where quarter-wave plates of alternately high and low refractive indices are put together. In the middle, two identical layers are joined to form the quarter-wave step, see Figure 1 (right).

The optical distances between the etches are exactly $\lambda_{\text{res}}/2$. Without the quarter-wave step, all the reflected waves will therefore have the same phase and the resonant wavelength will be reflected instead of transmitted. With the quarter-wave step the reflected waves from the two sections will cancel each other, causing the wave to be completely transmitted.

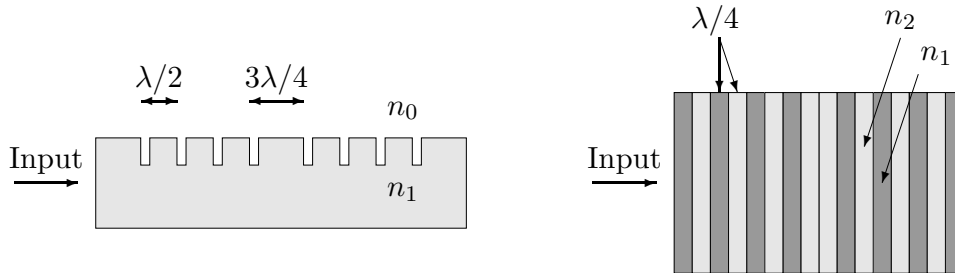


Figure 1: The grating resonance filter (left) and the Fabry-Perot interference filter (right). Note the quarter-wave displacements in the middle of the filters.

3.2 Approximation in one dimension

An approximative simulation of the optical filter can be made by solving the Helmholtz equation in one dimension using the discretization in Section 2.2. The gratings are modeled by variations in the wave propagation speed. This corresponds to normal incidence in the Fabry-Perot interference filter, although the width of the etches does not necessarily need to be a quarter of the wavelength. This approximate calculation will also be motivated by the results in Section 4.4, where we will see how an equivalent one-dimensional filter can be computed from a more realistic two-dimensional representation.

The actual values of the wave propagation speed in the etches are quite arbitrary, the desired effect will be observed as long as reflections occur. However, the fewer etches, the larger reflections are required to get a sharp resonance peak.

Now, by solving the Helmholtz equation for different values of the wave number k , a spectrum of the transmitted intensity can be plotted. This is done in Figure 2, with and without the quarter-wave displacement. The wave numbers k are normalized with respect to the resonant wave number k_{res} according to

$$k_{\text{norm}} = \frac{k - k_{\text{res}}}{k_{\text{res}}}. \quad (24)$$

The resonance effect is indeed very evident in this example, even though only 24+24 etches are used. In reality, as we will see in the next section, the resonance peak will not always be this sharp with so few etches.

In Figure 3 the real part of the solution is shown for two different cases, at the resonant frequency and at a slightly lower frequency where almost no intensity is transmitted. Note that the amplitude inside the filter at resonance is much larger than the incoming amplitude, because of the interference effects.

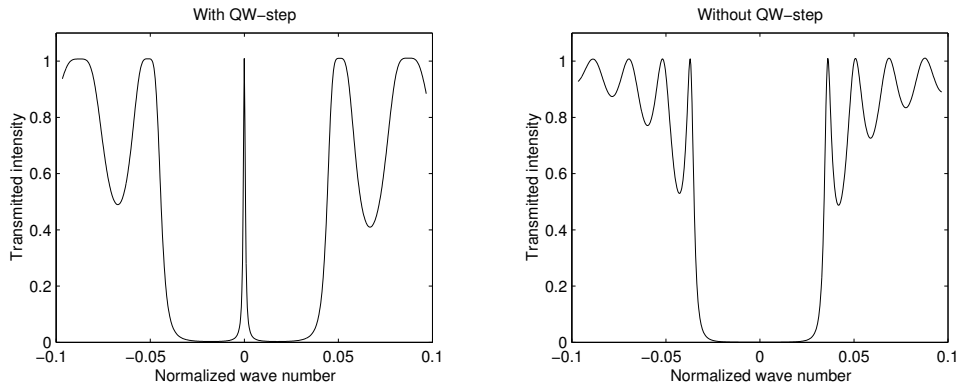


Figure 2: Spectrum from the one-dimensional simulation of the optical filter, with and without the quarter-wave displacement.

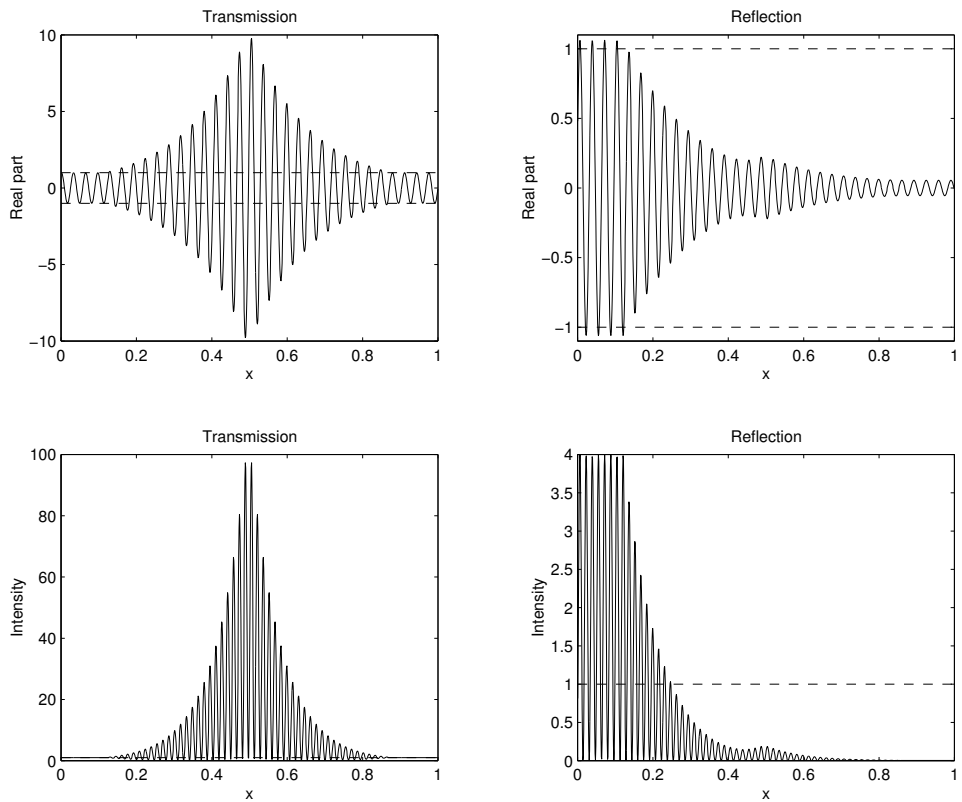


Figure 3: Real parts and intensities of the solutions for two different frequencies, the resonant frequency (left) and a slightly lower frequency (right). Note the large amplitudes inside the filter at resonance.

3.3 Two-dimensional calculations

Although there are a lot of similarities between the Fabry-Perot interference filter and the grating resonance filter, there are still questions unanswered by the one-dimensional calculations in the previous section. For instance, what influence does the grating depth have on the solution²? If the etches would cover the whole cross-section, then it is clear that the results would be similar to the one-dimensional case. But with smaller etches, the wave will change direction of propagation when interacting with the gratings, and the situation will become much more complicated. As we will see, the width of the waveguide will affect the solution as well.

By simulating the optical filter in two dimensions, the true geometry of the waveguide, Figure 1 (left), can be represented. Using the methods described in Section 2.2, I have solved the Helmholtz equation for a two-dimensional model of the waveguide. Along the sides of the waveguide I have, somewhat arbitrarily, used a Neumann boundary condition. However, numerical experiments indicate that the character of the interference phenomena in the solution does not change much when more physically motivated boundary conditions are used.

In [9], the fabrication of an optical filter is described. In order to get a realistic design, I have tried to resemble this filter as much as possible. I assume the material of the waveguide to be GaAs with refractive index of $n \approx 3.3$ and the surrounding medium to be vacuum. The width of the waveguide is three resonant wavelengths and the number of etches a few thousands. The spectrum of the transmitted intensity for this geometry is shown in Figure 4 (left).

A clear resonance peak appears even in this spectrum, although it is not as distinct as in the one-dimensional case. The reason for this is, as previously indicated, that the waves are allowed to propagate in different directions along the waveguide, which results in a much less efficient interference. This can to some extent, as in my simulations, be compensated for with an increased number of etches.

From this description, it is easy to understand that the width of the waveguide has a very large influence on the performance of the filter. With a thinner waveguide the wave will not be permitted to bounce back and forth between the sides, and the interference between the reflected waves will be more efficient. The result is a sharper resonance peak, as can be seen in Figure 4 (right) where the spectrum is shown for a waveguide of width $\lambda_{\text{res}}/2$ and only 6+6 etches, but with the same geometry of the etches as before. The ripple in this spectrum is likely due to numerical errors.

The solutions to the two-dimensional calculations are easily visualized with a gray scale plot of the absolute amplitude. In Figure 5, this is shown

²Discussions of the influences of the etch depth and the etch width are given in [13] and in [12].

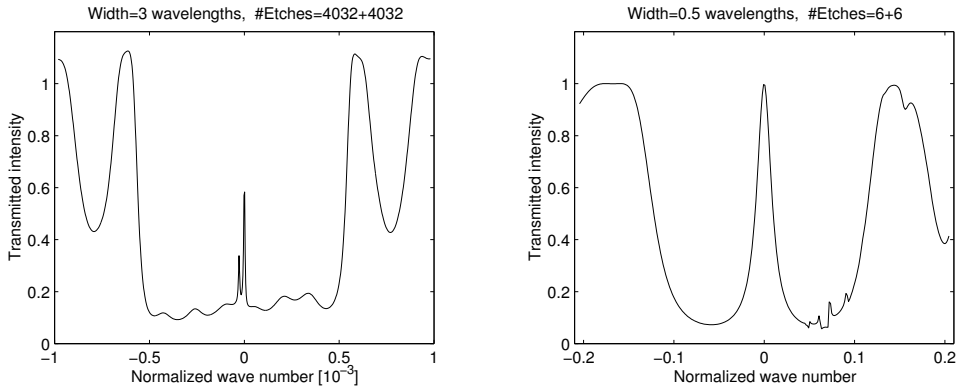


Figure 4: Spectra from the two-dimensional simulations. Left: A wide waveguide with thousands of etches. Right: A thin waveguide with only 6+6 etches. The interference is much more efficient for thin waveguides.

for the filter with 6+6 etches at two different frequencies. For comparison with the one-dimensional solutions in the previous section, Figure 3, I have also included plots of the intensities in the cross-sections. The similarities show that it is the same phenomena that occurs in the two simulations, and that the Fabry-Perot interference filter indeed is a special case of the grating resonance filter.

4 Wavelet homogenization

In many problems, large structures that contain fine details need to be modeled. The details must be resolved in order to get a correct solution, but the computations become too extensive with a small grid-size. In [4] and [1], the method of *wavelet-based numerical homogenization* was presented as a general tool to deal with this multiple scale problem. The idea of the numerical homogenization is to construct operators acting on coarse grids, but with the sub-grid phenomena included.

I have applied the wavelet homogenization on the optical filter from Section 3, which is a large-scale system (the whole waveguide) with fine-scale structure (the individual etches).

4.1 Theory

In this section I will limit myself to a brief description of the practical procedure of wavelet homogenization using the Haar-basis. More detailed treatments, including two-dimensional extensions, can be found in [4] and [1].

In the Haar system, the *shape function* $\varphi(x)$ and the *mother wavelet* $\psi(x)$ are given by (see Figure 6)

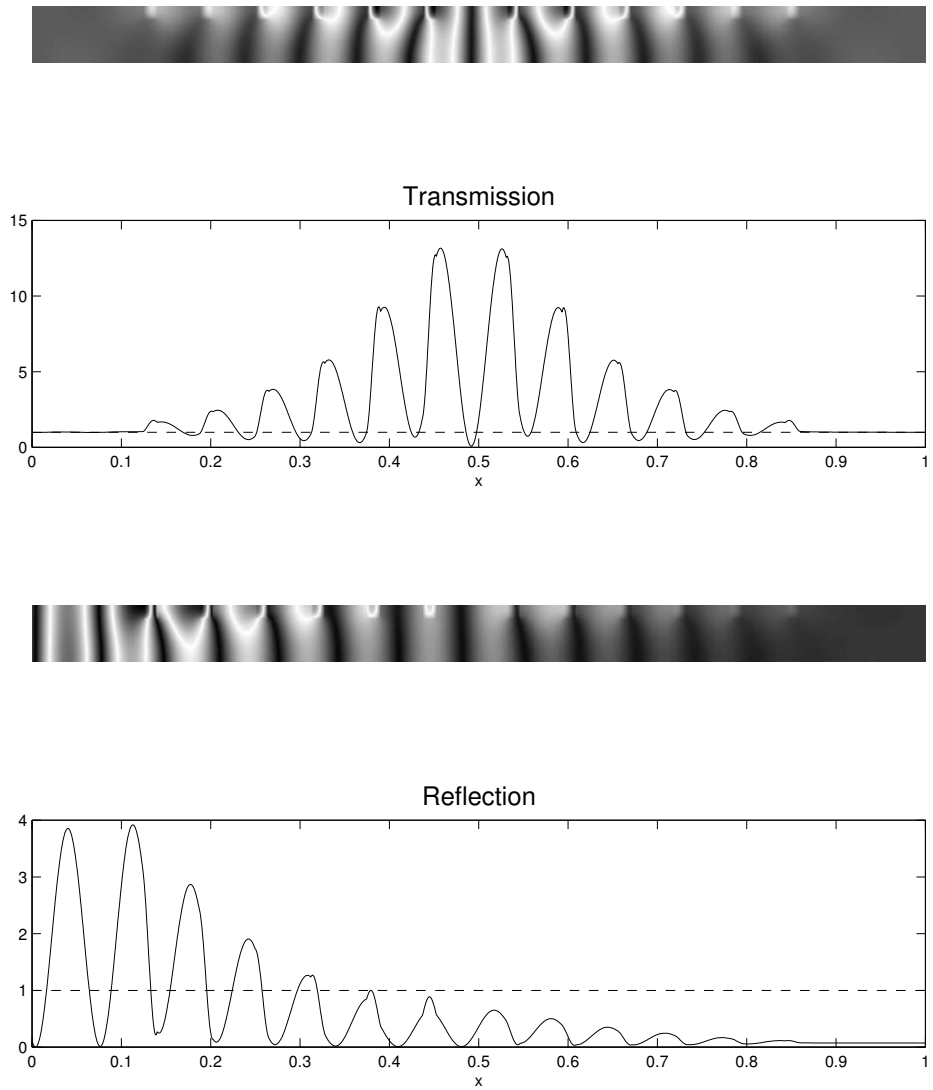


Figure 5: Two-dimensional solutions to the optical filter for two different frequencies. Plots of the intensities in the cross-sections are also included.

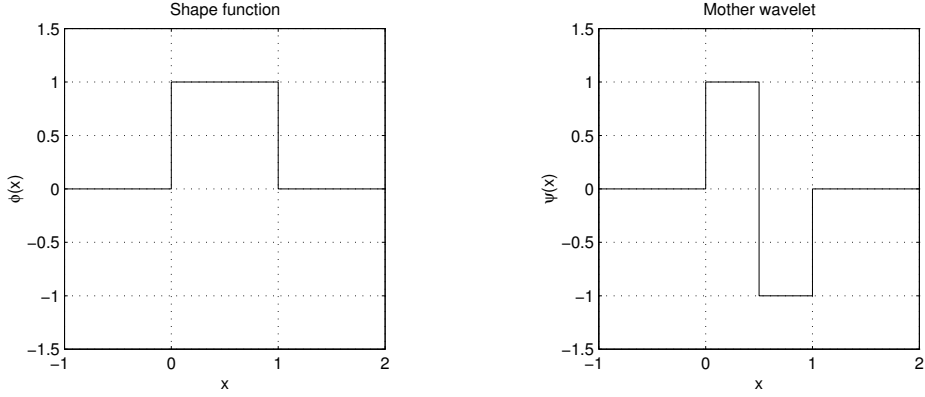


Figure 6: The shape function and the mother wavelet in the Haar-basis.

$$\varphi(x) = \begin{cases} 1, & \text{if } 0 \leq x \leq 1, \\ 0, & \text{otherwise,} \end{cases} \quad \psi(x) = \begin{cases} 1, & \text{if } 0 \leq x \leq 1/2, \\ -1, & \text{if } 1/2 \leq x \leq 1, \\ 0, & \text{otherwise.} \end{cases} \quad (25)$$

Let \mathcal{W} be the orthogonal transformation that corresponds to one step in the discrete Haar-basis wavelet transform. It has the following matrix representation,

$$\mathcal{W} = \frac{1}{\sqrt{2}} \begin{pmatrix} 1 & -1 & 0 & \cdots & & \\ 0 & 0 & 1 & -1 & 0 & \cdots \\ \vdots & \vdots & & \ddots & \ddots & \\ 0 & 0 & \cdots & 0 & 1 & -1 \\ 1 & 1 & 0 & \cdots & & \\ 0 & 0 & 1 & 1 & 0 & \cdots \\ \vdots & \vdots & & \ddots & \ddots & \\ 0 & 0 & \cdots & 0 & 1 & 1 \end{pmatrix}. \quad (26)$$

Applying the transformation \mathcal{W} on a vector U will have the effect of extracting the high and the low frequency parts U_h and U_l ,

$$\mathcal{W}U = \begin{bmatrix} U_h \\ U_l \end{bmatrix}. \quad (27)$$

Similarly, a linear operator L_{j+1} acting on a fine subspace can be decomposed into four operators A_j , B_j , C_j and L_j according to

$$\mathcal{W}L_{j+1}\mathcal{W}^\top = \begin{bmatrix} A_j & B_j \\ C_j & L_j \end{bmatrix}. \quad (28)$$

The operator L_j is the low frequency part of L_{j+1} , but does *not* in itself include the influence of high frequency phenomena. The object of the wavelet

homogenization is to construct an operator \bar{L}_j acting on the same coarse subspace as L_j , but with the fine-scale structure taken into account.

Now consider a system of linear equations

$$L_{j+1}U = F \quad (29)$$

like for instance the one in (11). Applying the wavelet transformations, we have

$$\mathcal{W}L_{j+1}\mathcal{W}^\top (\mathcal{W}U) = \mathcal{W}F \quad (30)$$

or, with the notations in (27) and (28),

$$\begin{bmatrix} A_j & B_j \\ C_j & L_j \end{bmatrix} \begin{bmatrix} U_h \\ U_l \end{bmatrix} = \begin{bmatrix} F_h \\ F_l \end{bmatrix}. \quad (31)$$

Finally, U_l can be determined by Gaussian elimination,

$$(L_j - C_j A_j^{-1} B_j) U_l = F_l - C_j A_j^{-1} F_h \quad (32)$$

and the homogenized large-scale operator \bar{L}_j , as well as the homogenized right hand side \bar{F}_j , is identified as

$$\bar{L}_j = L_j - C_j A_j^{-1} B_j, \quad (33)$$

$$\bar{F}_j = F_l - C_j A_j^{-1} F_h. \quad (34)$$

The procedure can be applied recursively to get operators acting on even coarser subspaces. The solution to each of the homogenized systems will be identical to the solution to the original system (29) projected on the coarse scale subspace.

4.2 Homogenization of optical filter

In this section I have applied the wavelet homogenization technique on the one-dimensional optical filter from Section 3.2. In Figure 7, the operator is shown at the resonant frequency after three homogenizations together with a close-up of the quarter-wave step.

The most apparent property of the operator is that the elements are concentrated to a band along the diagonal of the matrix. The physical interpretation of this is that an etch only interacts with its closest neighbors, it does not “sense” what happens a few wavelengths away. Hence, the homogenized operator is strongly diagonally dominant and essentially local. In that respect it retains the form of the unhomogenized operator, which is tridiagonal. The periodical structure of the gratings can be seen in the operator, as well as the quarter-wave step in the middle.

If homogenization is to be a useful technique for calculations on the optical filter, it is important that

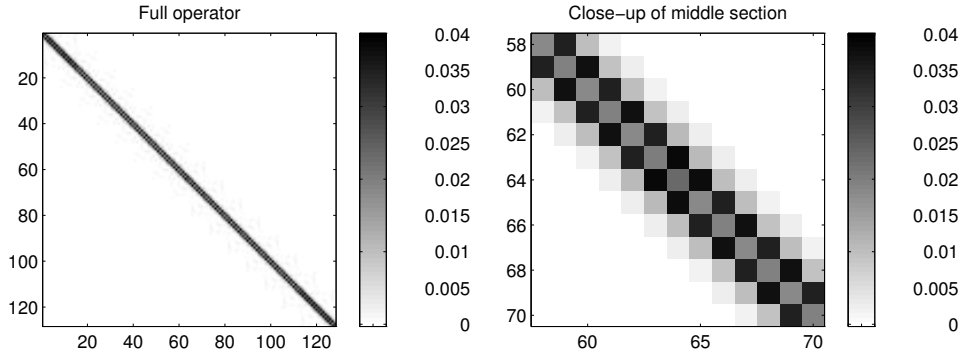


Figure 7: The full one-dimensional homogenized operator and a close-up of the quarter-wave step. The operator is strongly diagonally dominant, and it can be truncated to a bandwidth of $20+20$ without losing accuracy in the solutions.

- The homogenized solution gives an accurate value of the transmitted amplitude.
- The homogenized operator can be approximated by a sparse operator, for all fixed frequencies.

To see if the first demand is met, I have calculated the same spectrum as in Figure 2 after 1-3 homogenizations. This corresponds to 16, 8 and 4 points per wavelength. With further homogenization the oscillations would not be resolved, and then it is obvious that the results would be inaccurate.

The spectra are shown in Figure 8 (left). The homogenized solution consists of the mean values of the adjacent values in the original solution, therefore the slight reduction of the transmission ratios was expected. But the results are good enough for most purposes, even for the most homogenized case.

In order to investigate how the sparsity of the homogenized operator depends on the wave number k , a suitable measure of the concept sparsity is needed. To keep things simple, I will plot the sum of the absolute values in each diagonal. In Figure 8 (right) this is done for three values of k including the resonant wave number, and the resonance phenomena does not seem to influence the structure of the operator at all.

To summarize, homogenization of the optical filter preserves most of the interesting resonance properties, including the filter effect, and the operators can be approximated by sparse matrices regardless of the frequency. If the homogenization is made efficient, for example by implementing the *incomplete LU-factorization* [6], the total solution procedure using homogenization can be computationally as expensive as without it. However, large gains can be made if homogenized blocks are reused many times, and in the next section I will show how this can be done for the optical filter.

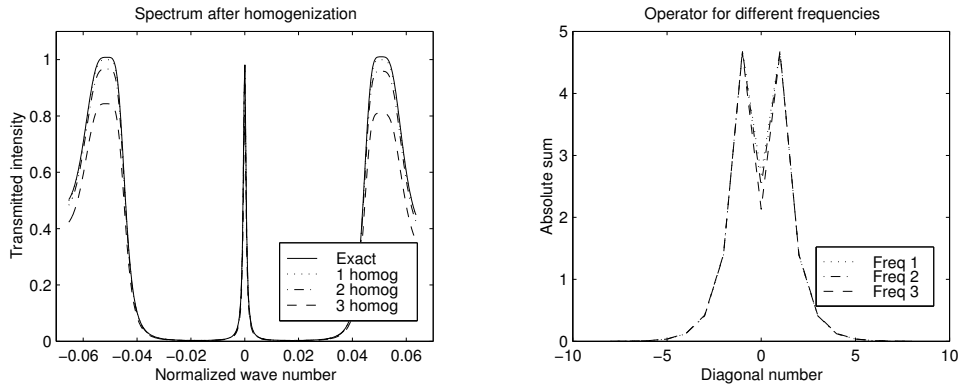


Figure 8: Left: Spectrum after 0-3 homogenizations. The resonance properties of the filter are preserved after homogenization. Right: Plots of the sum of the absolute diagonal values in the operator for three different frequencies, showing that the sparsity is essentially independent of the interference phenomena.

4.3 Extending periodical structures

The fact that the periodical structure of the optical filter is seen in the homogenized operator, and that the etches only interact within a limited range, can be very useful. It means that it is sufficient to homogenize a certain number of etches, and then all the other etches will have the same representation in the matrix.

The principle is illustrated in Figure 9. Two filters that are identical apart from the number of etches are homogenized three times each. In the final operator there are four points per wavelength, hence two points per etch. In the plots of the operators, especially in the diagonal plots, it can be seen that the etches are represented the same in the two cases, and so are the quarter-wave step and the leading and trailing sections. The element-values in the blocks are identical for the two operators, apart from the numerical deviations. Therefore, the larger case can be constructed by “copying and pasting” etches in the smaller matrix. In this way, it is possible to construct an operator representing a filter with an arbitrary number of etches.

The method makes it possible to compute the solution to a filter with a lot of etches on a coarse scale without computing the homogenization to the complete filter. To show that the method gives correct solutions, I have applied it to a case with thousands of etches with complex geometry, and verified that the homogenized solution is identical to the exact solution (after projection on the coarser subspace).

Note that it is not possible to homogenize each part of the waveguide separately and then assemble the homogenized blocks. The etches, the quarter-wave step and the leading and trailing sections must be homoge-

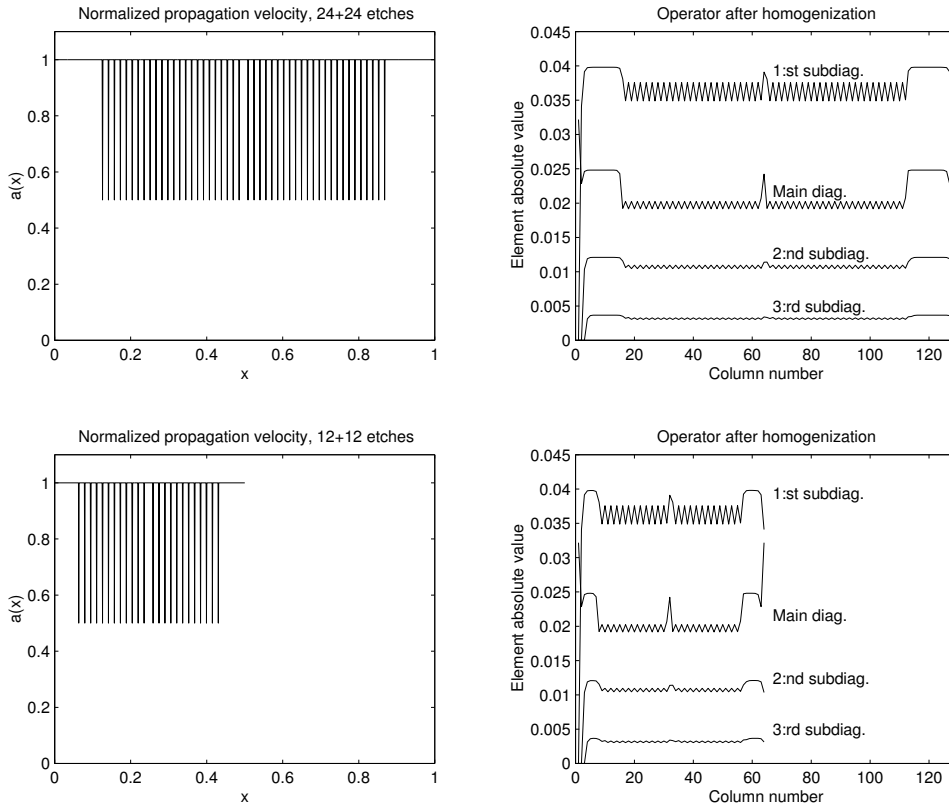


Figure 9: Two filters with the same geometry, but with different numbers of etches are homogenized (left). The diagonal plots of the operators (right) show that the blocks are represented the same, and operators representing filters of arbitrary sizes can therefore be constructed.

nized together. Otherwise the high frequency interaction between the blocks would be lost, which would result in an incorrect solution. The minimum bandwidth that can be accepted determines the number of etches that must be homogenized.

If the structure had been completely periodical, then *classical homogenization* [2] would have predicted the correct solution in a very simple manner. But in order to simulate a situation with blocks of partly periodical structures, where the blocks have high frequency interactions, classical homogenization cannot be applied. Here, wavelet homogenization works well, because of wavelets' good ability to approximate local properties. The representation of the structures and the interaction between them can be seen clearly in the operators. However, the bandwidth of the matrix increases after homogenization and for the method to yield significant gains in efficiency, it need to be generalized to higher dimensions.

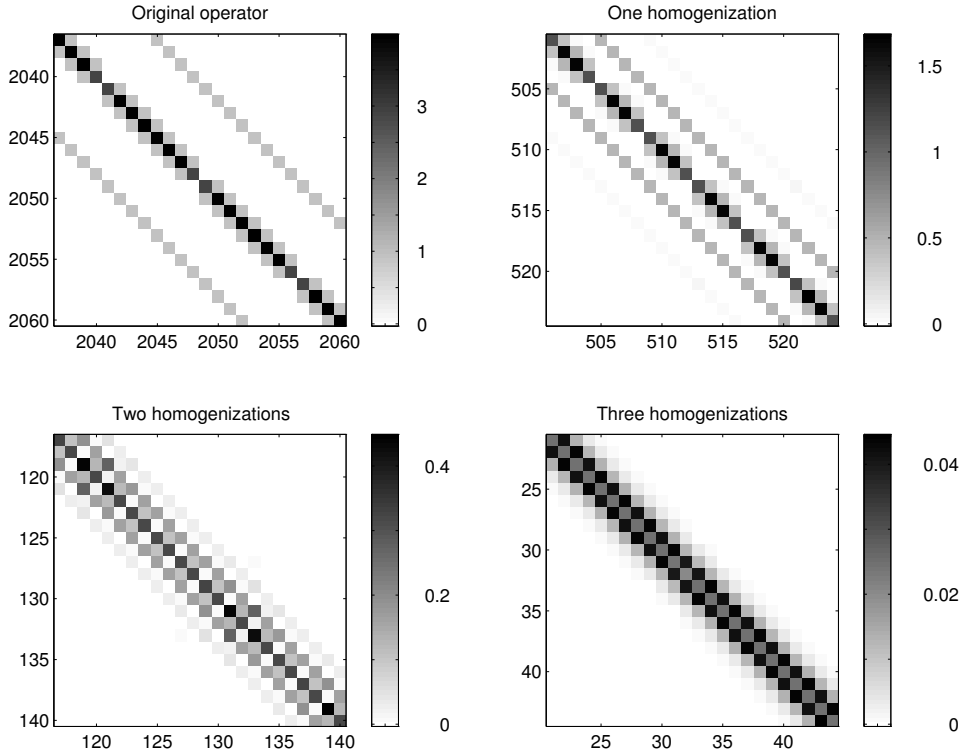


Figure 10: Sections of the two-dimensional operator after 0-3 homogenizations.

4.4 Homogenization in two dimensions

The two-dimensional models of optical filters in Section 3.3 are very well suited for numerical homogenization. The variations of the solution within the cross-section are of no interest, and thus they need not be resolved. Multiple homogenizations can be applied to reduce the number of points in the cross-section to a single one, and thereby create an equivalent one-dimensional model of the problem. As before, the wavelength must still be resolved in the direction of propagation.

There is a lot to be gained computationally by homogenizing the two-dimensional operators. The bandwidth does not grow as much after homogenization as it did in the one-dimensional case. Depending on the desired accuracy, the bandwidth can sometimes even be diminished. Furthermore, the homogenized operator is of the same kind as the one-dimensional operators in Section 4.2, and therefore the technique from Section 4.3 of extending periodical structures can be applied here as well.

In Figure 10, operators corresponding to a two-dimensional optical filter are shown after different numbers of homogenizations. The filter has approximately the same geometry as the filters in Section 3.3, the number of

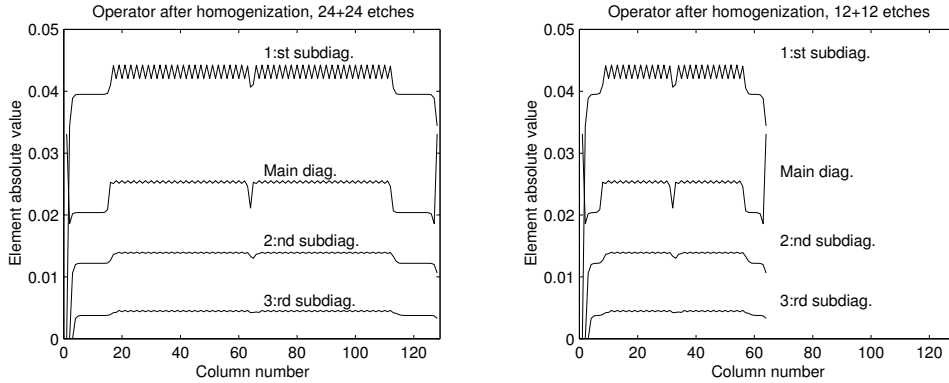


Figure 11: The two-dimensional correspondence to Figure 9, showing that the “copy and paste”-technique can be used even in this case.

etches is 24+24 and the width of the waveguide is one wavelength. Note how the main diagonal band is broadened after homogenization while the outer sub-diagonals approaches the main diagonal, resulting in an essentially unchanged bandwidth.

To show that the “copy and paste”-technique still is applicable, I have made the same calculations as in Section 4.3 but in two dimensions. Two filters, identical apart from the number of etches, have been homogenized to the same extent. Plots of the main-diagonal and some sub-diagonals are shown in Figure 11.

The similarities with Figure 9 imply that the periodical structures can be extended in this two-dimensional case as well, and a more detailed analysis shows that the method gives accurate results. Furthermore, the homogenized two-dimensional operator can be interpreted as an equivalent one-dimensional operator, and this motivates the approximative calculation in Section 3.2.

5 Conclusions

The simulation of optical filters is a good example of the practical use of wavelet homogenization. Below, the main properties of the filter that make it especially suitable for homogenization are listed.

- The geometry contains fine-scale details that affect the coarse-scale solution.
- The solution does not need to be resolved in all space dimensions.
- The geometrical structure contains sections with identical blocks periodically repeated.

The techniques I have described in this report can be applied to a lot of other problems with the above properties, in order to reduce the computational effort significantly.

6 Acknowledgements

I would like to thank my thesis advisor, Professor Björn Engquist, and Professor Jesper Ooppelstrup for their most valuable advice. I am greatly indebted to Olof Runborg for his efforts and commitment. I am also grateful to my examiner, Professor Gustaf Söderlind, and to the staff at PDC, the Center for Parallel Computers at KTH.

References

- [1] Ulf Andersson, Björn Engquist, Gunnar Ledfelt, and Olof Runborg. Wavelet-Based Subgrid Modeling: 1. Principles and Scalar Equations. Technical report, C²M², NADA, KTH, 1996.
- [2] A. Bensoussan, J. L. Lions, and G. Papanicolaou. *Asymptotic Analysis for Periodic Structures*. North-Holland Publishing Company, 1978.
- [3] David K. Cheng. *Field and Wave Electromagnetics*. Addison-Wesley Publishing Company, Inc., 1989.
- [4] Mihai Dorobantu and Björn Engquist. Wavelet-Based Numerical Homogenization. Technical Report TRITA-NA-9601, C²M², NADA, KTH, 1996. Accepted in SIAM J. Num. Anal.
- [5] Dan Givoli. *Numerical Methods for Problems in Infinite Domains*. Elsevier Science Publishers B.V., 1992.
- [6] Gene H. Golub and Charles F. Van Loan. *Matrix Computations*. The John Hopkins University Press, 1996.
- [7] Hermann A. Haus and Y. Lai. Narrow-Band Optical Channel-Dropping Filter. *Journal of Lightwave Technology*, 10(1):57–61, January 1992.
- [8] Eugene Hecht. *Optics*. Addison-Wesley Publishing Company, Inc., 1987.
- [9] M. Levy, L. Eldada, R. Scarmozzino, R. M. Osgood Jr., P. S. D. Lin, and F. Tong. Fabrication of Narrow-Band Channel-Dropping Filters. *IEEE Photonics Technology Letters*, 4(12):1378–1381, December 1992.
- [10] William H. Press, Saul A. Teukolsky, William T. Vetterling, and Brian P. Flannery. *Numerical Recipes in C*. Cambridge University Press, 1992.
- [11] Gilbert Strang. *Introduction to Applied Mathematics*. Wellesley-Cambridge Press, 1986.
- [12] Lawrence C. West, Charles Roberts, Jason Dunkel, Gregory Wojcik, and Jr. John Mould. Non Uniform Grating Couplers for Coupling of Gaussian Beams to Compact Waveguides. *Integrated Photonics Research Technical Digest, Optical Society of America*, 1994.
- [13] G. Wojcik, J. Mould Jr., and L. C. West. Time-Domain Finite Element Modeling of 3D Integrated Optical Devices. *Integrated Photonics Research Technical Digest, Optical Society of America*, 1993.